行政院國家科學委員會補助專題研究計畫成果報告

※※※※※※※※※※※※※※※※※※※※※※※※※※※

※ 三唯全像光學記憶系統的製作及其整合研究-子計畫-二: ※
※　　微振鏡機制之設計、分析、製作與測試之研究　　※
※　　　　　　　　　　　　　　　　　　　　　　　※

※※※※※※※※※※※※※※※※※※※※※※※※※※

計畫類別：□個別型計畫　　■整合型計畫
計畫編號：NSC 89-2215-E-009-125
執行期間：89 年 8 月 1 日至 90 年 7 月 31 日

計畫主持人：邱俊誠 教授
共同主持人：吳炳飛 教授

本成果報告包括以下應繳交之附件：
　　□赴國外出差或研習心得報告一份
　　□赴大陸地區出差或研習心得報告一份
　　□出席國際學術會議心得報告及發表之論文各一份
　　□國際合作研究計畫國外研究報告書一份

執行單位：交通大學 電機與控制工程學系

中　華　民　國　　90　年　10　月　25　日

行政院國家科學委員會專題研究計畫成果報告
The Design, Analysis, Fabrication and Testing of Micromirror
微振鏡機制之設計、分析、製作與測試之研究

Abstract

In this report, the configuration of combining holographic gratings and micromirror devices for optical add/drop functions is proposed for constructing OADM. Based on this architecture, a MEMS-based vibrating micromirror device that is driven by electrostatic force in executing add/drop functions is designed and fabricated. Preliminary experiments had demonstrated the feasibility of the proposed system.

Keywords: Micromirror, Holographic Gratings, OADM, Optical MEMS

中文摘要

本計畫研究重點在於擁有一維自由度光切換元件的機構設計、分析與模擬。此元件將可應用於高密度分波多工器上。在此已完成驅動控制方式設計、製程設計，光罩佈局，元件製作、元件的量測與動態特性分析等工作。

關鍵詞：微振鏡、全像光柵、高密度分波多工器、光微機電

1. INTRODUCTION

For a Dense Wavelength Division Multiplexing (DWDM) networking system, Optical Add/Drop Modules (OADM), that play important role both in optical core networks and in regional access networks, are often required for optical communication. The OADM selectively removes (drops) a wavelength from a multiplicity of wavelengths in a fiber, and adds in the same direction of data flow the same wavelength, but with different data content. Through the OADM modules, the specific data or information could be extracted from or carried into the DWDM networking system such that information could be received or transmit among each communication nodes [1].

To achieve division/collection of the optics in the fiber, narrowband spectral filters are always used for demultiplexing (DMUX) and multiplexing (MUX) functions. There are several approaches for these filter modules in the WADM, including fiber grating based reflection filters, Fabry-Perot filters, thin film interference filters, Mach-Zehnder filters, birefringent filters, and arrayed wave-guide grating [1]. In general, different filter configuration has its own advantages and drawbacks. In this paper, the volume holographic filter that has narrow-pass-band nature of the light wavelength due to the Bragg condition is used [2]. The high signal-to-noise (S/N) ratio, high insertion efficiency, compact structure, and very narrow-pass-band make these gratings be the potential components for next generation DWDM devices.

Microelectromechanical System (MEMS) devices are being widely developed for various optical applications in the last decade. Based on this technology, the passive and active optical components such as mirrors, lens, gratings and even laser diode or VCSEL are now capable of integrating onto a single chip. The system would be developed compactly with low cost and enhanced performance. In this paper, a micromirror device based on MEMS technology is presented and demonstrated for OADM realization. Electrostatically-driven method is

used to approach high frequency operation of the mirror. The configuration combined with holographic gratings and micromirror devices is proposed for optical add/drop functions. The principle of the volume gratings and design, analysis of the micromirror device would be presented and described. The preliminary experimental results had also been demonstrated for the feasibility of the OADM.

2. Optical add/drop module configuration

A typical OADM usually consist of two major components: filter modules, and optical switches. As shown in Figure 1, incidence lights with different wavelengths are coupled into DMUX. Then each wavelength will be diffracted into its designed position by the corresponding holographic volume grating. These gratings are multiplexed by the localized multiplexing method, which can provide much higher diffraction efficiency of each hologram in the same volume of the recording material [3]. The back-to-back micromirror array is used for dropping specific wavelength outputted from the DMUX, and adds desired wavelength signals into MUX channels. The MUX device also contains a series of localized-multiplexed volume holographic gratings, in which the Bragg condition of each grating is set identically as the corresponding channel of the DMUX device such that MUX device collect all signal channels and then start next journey through the fiber. When both mirrors in the optical path are turned off, the light can pass through DMUX and MUX, and then into next fiber. Combining those functions, the OADM prototype could be obtained.

2. 1 Volume holographic gratings

In general, optical filters using volume holographic gratings are based on the Bragg diffraction, in which wave with the specific wavelength can be diffracted from the phase grating as it meet the Bragg condition and the others transmit directly. Therefore, superimposing multiple volume gratings each with specific Bragg conditions in a holographic material by using multiplexing technologies is an essential and compact structure to form DMUX and MUX devices. Referring to Fig. 1, we use the localized multiplexing technique to achieve the high diffraction efficiency requirement. On recording, each wave with different wavelength is respectively introduced form both adjoin surfaces of the recording light entree and the fiber end. On reconstruction, because all waves from the fiber enter the DMUX simultaneously, each channel diffracts not only the corresponding wavelength but also all other wavelengths under Bragg-mismatched conditions. As a result, these Bragg-mismatched reconstructions produce the noise of each channel. The amount of phase-mismatched is roughly proportional to the wavelength separation between the original recording wave and all other waves. For the ith channel the amount of phase-mismatch is $\Delta k = 2\pi(m-i)\delta\lambda/(\lambda_m\lambda_i)$ from the mth recording wavelength. Assuming the diffraction efficiency of each grating remain the same value, the noise-to-signal ratio of ith channel, derived by the coupled wave model [3], is proportional to

$$\sum_{m \neq i} \text{sinc}^2\left(\frac{\Delta k L}{2\pi}\right) \qquad (1)$$

where $\text{sinc}(x)=\sin\pi x/(\pi x)$, $\delta\lambda$ is the standard deviation of wavelength for DWDM and L is dimensional size along the normal of the recording wave. It follows by choosing the dimensional size L such that the sinc function of Eq. (1) vanishes, the noise will be eliminated, leaving a clean signal. From Eq. (1) the minimal required size L is

$$L \approx \frac{\lambda_m\lambda_i}{(m-i)\delta\lambda} \qquad (2)$$

Having eliminated the noise from the finite

dimensional size L, we should examine noises resulting from the other channels due to the finite beam diameter D of the recording waves. Using the Fourier optics, the noise of ith channel from the other channel can be written as

$$\sum_{m \neq i} \text{sinc}^2 \left(\frac{D}{\lambda_m z_o} (m-i) \Delta \right) \qquad (3)$$

where z_o is the distance between the grating and the mirror, Δ is the spatial separation between the adjoin channels. Again, by choosing the proper parameters D and Δ, the sinc function in Eq. (3) can be minimized, even vanished, leaving a clean signal. The minimal required channel separation is

$$\Delta \approx \frac{\lambda_i z_o}{D} \qquad (4)$$

Therefore, using the Eqs. (1-4), we can design and analyze the both DMUX and MUX in the OADM according to the system requirements.

3. Micromirror design

To realize the proposed OADM configuration as shown in Fig. 1, the back-to-back micromirror array is designed and analyzed. Here the designed requirement for the micromirror device is concentrated on the capability of large out of plane rotating angle and a mechanism that can enforce the micromirror to stay on the designed flip-up angle.

To achieve this goal, the micromirror design is fabricated through MUMPs [4]. The micromirror device that consists of a set of two back-to-back micromirrors (diameter = 200um), micro-hinges, four pre-stressed beams and restoring beams are shown in Figs. 2 and 3. The metal layer (Gold) is deposited on the center of two mirrors to obtain high reflect efficiency.

In order to minimize curvature of the mirror surface due to residual stress, the multi-layer structure design had been used [6]. The 0.75um oxide layer (PSG2) was trapped between two polysilicon layers (Poly1 and Poly2) of MUMPs. To realize this optical reflect efficiency, no etching holes are used on the mirror of 200um in diameter. Fig. 4 shows the surface profile of the micromirror device using interferometer microscope. It is clearly shown that the curvature of mirror is less than 2um across the surface.

Pre-stressed beam designed from residual stress of multi-layers had been proposed for some applications [5]. Here, we use this concept to generate vertical displacement to flip-up micromirror after release process. Simulations using commercial FEM software IntelliSuite$^{\text{TM}}$ had been carried out to predict actuating force. As shown in Fig. 5, the tip on the free end of the beam would generate several um displacement or approximately a few uN force depending on the residual stress generated during process. In the presented paper [5], the design dimension size of the pre-stressed beam had been described and discussed in detail. Here, Table 1 shows the simulation parameters that we used for OADM micromirror design.

Note that the pre-stressed beam has designed to activate vertical displacement of the flip-up mirror whereas the restoring beam is designed to ensure the contact of the mirror after it has flip up. As shown in Fig. 6, the restoring beam is experiencing bending as the pre-stressed beam is flipping up the mirror device. Note that during the transient condition, we observe that

$$F_{pre-stressed} > F_{restoring-beam} + F_{hinge} \qquad (5)$$

and for the steady state, we have

$$F_{pre-stressed} = F_{restoring-beam} \qquad (6)$$

where $F_{pre-stressed}$ and $F_{restoring-beam}$ are the force generated by pre-stressed beam and by

restoring beams respectively, and F_{hinge} is the friction force of the micro-hinge.

Finally, by adopting the standard release process in removing the sacrificial layers, and supercritical point drying process for sticking prevention, the micromirror is initially flipping out of plane as shown in Fig. 7. By applying the driving voltage on the pre-stressed beam and electrode under the beam, the mirror device can be pull-down in conjunction with the restoring beams. Here, the micromirror device could be operated to be out-of-plane or on the plane by controlling the driving voltage. Finally, the add/drop functions needed in the Fig. 1 configuration is obtained.

4. Experimental results

Fig. 8 illustrates the optical experimental configuration of switching micromirror devices for add/drop functions. A 650nm He-Ne Laser is used to be the incidence light source. Two mirrors and the lens with focal length of 50cm are used to focus light onto the micromirror device. The high-speed photodiode is used to detect the response characteristics of the micromirror. When the driving signals are applied to micromirror devices, the switching speed and the response performance could be measured.

Fig. 9 and 10 show the test and measurement results of the fabricated micromirror. It is clearly that the mirror device can switch the light into different directions depending on the applied signals. Figure 10 shows the switching speed of the fabricated micromirror reach 5ms with good transient characteristics. However, when the switching speed of the micromirror is increased from 20 Hz to 100 Hz, a chattering effect has been observed due to the dynamic characteristic of the pre-stressed beams.

5. Conclusion

A micromirror device for optical add/drop module had been presented in this paper. Based on the proposed configuration, the micromirror device could be integrated with holographic gratings to be OADM modules. Lights with different wavelengths are coupled into DMUX, and added by MUX. Designed back-to-back micromirror devices select the desired add/drop signals. Localized multiplexing technique of holographic gratings is used to achieve the high diffraction efficiency, and the electrostatically-driven method is guaranteed for high operation frequency. Through MUMPs process, some micromirror devices had been fabricated for system testing. Preliminary experiments had demonstrated the micromirror devices could be driven at 100Hz approximately. Moreover, some chattering effect generated by the pre-stressed actuators while driving at high frequencies had been also observed.

References

[1] S. V. Kartalopoulos, *Introduction to DWDM Technology*, SPIE, New York, 2000.

[2] L. Y. Lin, S. S. Lee, K. S. J. Pister and M. C. Wu, "Micro-machined three-diemnsional micro-optics for integratde free-space optical system," IEEE. Photonics Technol. Lett. 14, no. 12, 1445-1447, 1994.

[3] C. Moser, I. Maravic, B. Schupp, A. Adibi, and D. Psaltis, "Diffraction efficiency of localized holograms in doubly doped $LiNbO_3$ crystals," Opt. Lett. 25, 1243-1245, 2000.

[4] D. Koester, R. Mahedevan, K. Marcus, "Multi-User MEMS Processes (MUMPs) Introduction and Design Rules", rev. 3, http://www.memsrus.com, Oct, 1994.

[5] David C. Muller, Wenge Zhang, Victor M. Bright, "Microrelay Packaging Technology Using Flip-Chip Assembly", Proceedings of the 2000 IEEE International Conference on Microelectro- mechanical Systems (MEMS 2000), Miyazaki, Japan, pp. 265-270, January 23-27, 2000.

[6] A. Tuantranont, V. M. Bright, W. Zhang, J. Zhang, and Y. C. Lee, "Self-Aligned Assembly of Microlens Arrays with Micromirrors," Proceedings of the 1999 International Society for Optical Engineering (SPIE
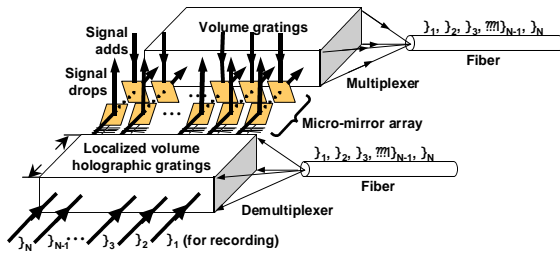
Fig. 1   OADM configuration
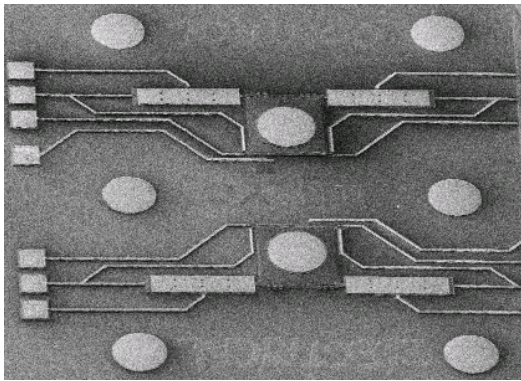
Fig. 2 SEM of the micromirror device
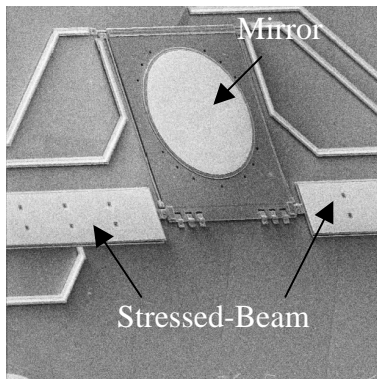
Fig. 3 Detail view of the mirror
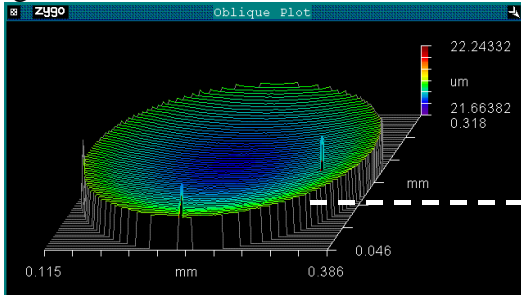
(a)
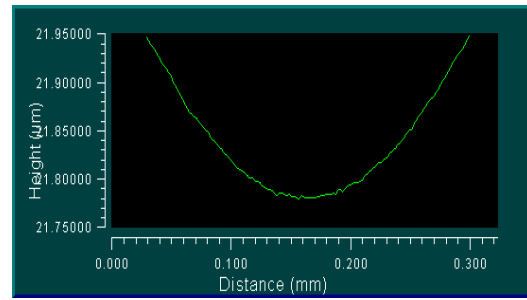
(b)

Fig. 4   The interferogram (a) and surface profile (b) of the reflective surface of the mirror
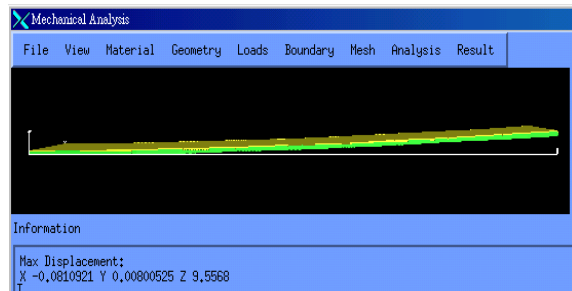
Fig. 5 FEM simulation of the pre-stressed beam

Table 1 FEM simulation parameters

	PolySilicon	**Gold**
Beam	300 um x 60 um	
Thichness	1.5 um	0.5 um
Young's Modulus	169 GPa	80 GPa
Density	2.3 g/cm^3	19.28 g/cm^3
Poisson Ratio	0.42	0.3
Stress	-7.4 Mpa	57.75 Mpa
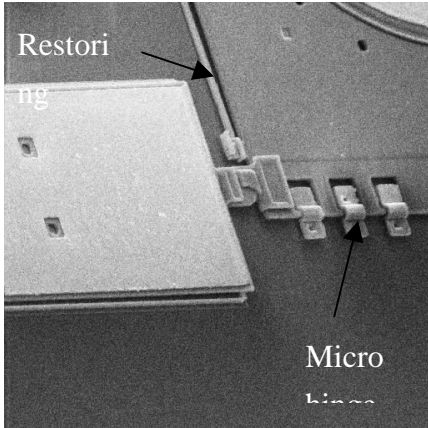
Fig. 6 SEM view of the restoring beam
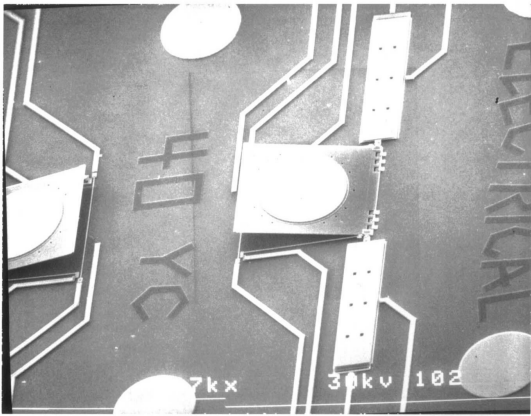
Fig. 7 Micromirror devices after release process
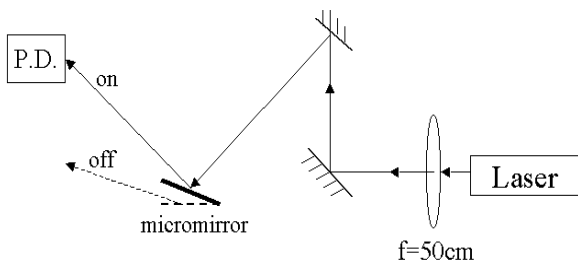
Fig. 8 Experimental configuration of the micromirror device

(a)

(b)
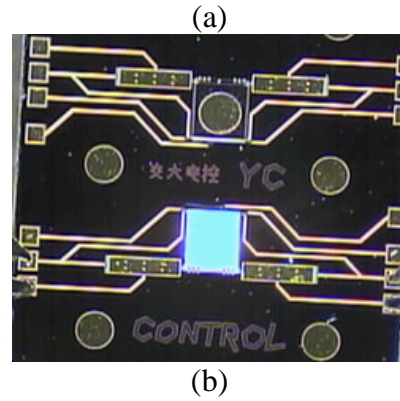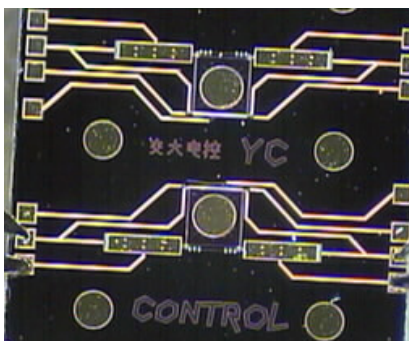
Fig. 9 (a) Both mirrors are actuated (In plane) (b) One of the mirrors is released (Out of plane)
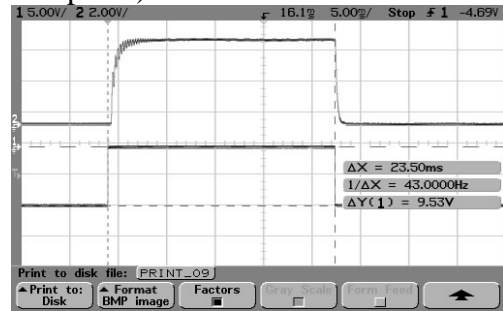
(a)
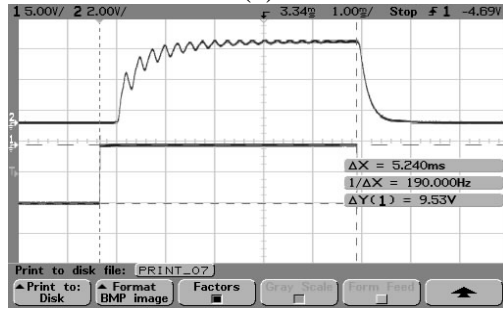
(b)

Fig. 10 (a) On-off response of the micromiror at 20Hz (b) On-off response of the micromiror at 100Hz